CircRNA circ-0110102 Function as Anti-oncogenic Gene in Hepatocellular Carcinoma through Modulating miR-580-5p/CCL2 Pathway

Xinxing Wang
Shandong Provincial Hospital
Wei Sheng
Shandong Provincial Hospital
Tao Xu
Shandong Provincial Hospital
Jiawen Xu
Shandong Provincial Hospital
Juntao Chen
Shandong Provincial Hospital
Zhonghou Rong
Shandong Provincial Hospital
Zhiyi Wang
Shandong Provincial Hospital
Dongdong Du
Shandong Provincial Hospital
Yadong Wang
Shandong Provincial Hospital
Ruyi Gao
Shandong Provincial Hospital
Zhenhai Zhang (zhangzhenhai0410@126.com)
Shandong Provincial Hospital

Research

Keywords: hsa_circ_0110102, miR-580-5p, CCL2, hepatocellular carcinoma, cyclooxygenase-2, prostaglandin E2

Posted Date: July 29th, 2020

DOI: https://doi.org/10.21203/rs.3.rs-49964/v1

Abstract

Background

Circular RNAs (circRNAs) have been shown to have critical regulatory roles in tumor biology, whereas their contributions in hepatocellular carcinoma (HCC) still remains enigmatic. The purpose of this study was to investigate the molecular mechanisms involved in hsa_circ_0110102 in the occurrence and development of HCC.

Results

hsa_circ_0110102 was significantly down-regulated in HCC cell lines and tissues, low hsa_circ_0110102 expression levels were associated with poor prognosis. Knockdown hsa_circ_0110102 significantly inhibited cell proliferation, migration and invasion. In addition, the interaction between hsa_circ_0110102 and miR-580-5p was predicted and verified by luciferase assay and RNA pull-down, indicating that hsa_circ_0110102 function as sponge of miR-580-5p. Moreover, miR-580-5p which could directly bind to the 3'-UTR of CCL2 and induce its expression, then active the COX-2/PGE2 pathway in macrophage via FoxO1 in p38 MAPK dependent manner. Furthermore, the Δ256 mutant of FoxO1 showed no activation effect. These results concluded that hsa_circ_0110102 act as a sponge for miR-580-5p and decreased CCL2 secretion in HCC cells, then inhibits pro-inflammatory cytokine release from activated macrophage by regulating the COX-2/PGE2 pathway.

Conclusions

These results indicating that hsa_circ_0110102 serves as a potential prognostic predictor or therapeutic target for HCC.

Introduction

Hepatocellular carcinoma (HCC) is the most frequent primary malignancy of the liver and the third leading cause of cancer death worldwide [1], which accounts for about 90% of all cases of primary liver cancers [2]. China accounts for more than 50% of the total HCC cases worldwide. The main risk factors for HCC are chronic infection with hepatitis B virus (HBV) and hepatitis C virus (HCV) and nonalcoholic fatty liver disease (NAFLD). Over the past decades, great efforts have made to reach diagnosis and treatment methods to new heights, but the mortality rate is still unsatisfactory. Therefore, it is urgently relevant to determine the risk factors of HCC occurrence and reveal the molecular mechanism of its promotion.

Circular RNAs (circRNAs) are a subclass of transcripts with covalently closed loop structures that lack classic 5' caps or 3' polyadenylated tails, which used to be regarded as by-products of erroneous splicing

[3, 4]. But recently, mounting studies have shown that circRNAs play important roles and serve various functions in nervous system, carcinogenesis, cardiovascular diseases, immunomodulation and metabolic disorder [5–8]. CircRNA could regulates target gene or protein expression in various manners[9]: function as microRNA (miRNA) sponges to show miRNA inhibition effect by competing endogenous RNA (ceRNA) [10], interfere with their parental genes by modulation of alternative splicing or transcription[11], and interact with RNA-binding proteins (RBPs) as scaffolds for the assembly of protein complexes [12]. Recently, numerous circRNAs have found to be dysregulated in HCC. For example, CircBACH1 (hsa_circ_0061395) is significantly upregulated in HCC tissue and circBACH1 knockdown suppresses the proliferation and increased apoptosis of HCC cells by regulating p27 repression via HuR[13]. CircASAP1 acts as a ceRNA for miR-326 and miR-532-5p to mediates tumor-associated-macrophage (TAM) infiltration [14]. As a consequence, emerging evidences support the critical roles of circRNA for HCC tumorigenesis and development.

C-C chemokine ligand 2 (CCL2) is overexpressed in HCC and is a prognostic factor for patients [15, 16]. In tumor microenvironment, the interaction between CCL2 and C-C motif chemokine receptor 2 (CCR2) could regulates chemotaxis of TAMs and contributes to the cancer progression. Cyclooxygenase-2 (COX-2), as the key enzyme in the synthesis of prostaglandin E2 (PGE2), is an important inflammatory factor and over-expressed in many metastatic tumors [17]. COX-2 plays an important role in angiogenesis, apoptosis, inflammatory and metastatic[18] and is proposed as a potential tumor therapeutic target [19]. Nonsteroidal anti-inflammatory drugs (NSAIDs), the main available COX-2 inhibitors, have been widely used in cancer treatment[20, 21].

In our study, we identified a novel circRNA hsa_circ_0110102 and investigated its biological roles in the HCC progress. hsa_circ_0110102 could target the miR-580-5p/CCL2 in HCC. Moreover, CCL2 secreted into the tumor microenvironment could induced the COX-2 expression and PGE2 release via FoxO1-dependent manner in macrophage, and then promote the proliferation of HCC cells. Overall, these findings indicate that hsa_circ_0110102 might act as novel biomarkers for HCC prognosis and promising therapeutic targets.

Materials And Methods

Reagents

Recombinant human CCL2 for cell treatments was obtained from R&D (#279-MC-050). AS1842856 (#344355) and phorbol 12-myristate 13-acetate (PMA, #P8139) were obtained from Sigma-Aldrich (St. Louis, MO, USA). SB203580 (#S1076), SP600125 (#S1460) and SCH772984 (S7101) was obtained from Selleck (Shanghai, China). Dual-Luciferase® Reporter Assay System (E1910) was from Promega (Madison, WI, USA). Simple ChIP Plus Sonication Chromatin IP kit (#56383) and Alexa Fluor 488 conjugated CD68 antibody (#24850) was purchased from CST (Beverly, MA, USA). Alexa Fluor 647 conjugated CCR2 antibody (#ab225432) was obtained from Abcam (Cambridge, UK). Lipofectamine 2000 (#11668019), negative control (miR-NC), miR-580-5p mimic (#4464066) and inhibitor (AM17000)

were obtained from Thermo Fisher Scientific. siRNA-ZNF562, siRNA-circ-102231 and the negative control were purchased from GenePharma Biotechnology (Shanghai, China). The siRNA target site of hsa_circ_0110102: 5'-ACAGTGGAGAAAGGTAAATGCAA-3', siRNA target site of ZNF562: 5'-GTCATTGATAACATCTTATCAGG-3'. The construction of overexpressing hsa_circ_0110102 in Ubi-MCS-Luc-IRES-Puromycin vector was performed by Biosyntech Co., Ltd (Suzhou, China).

Clinical tissue samples and cell culture

HCC tissues used in this study involved 17 patients of both genders with previously diagnosed HCC (13 men, 4 women) with averaged age 57 ± 12 years at Shandong Provincial Hospital Affiliated to Shandong First Medical University, Jinan, China. Tumor tissues and adjacent tissue samples were immediately collected and placed into liquid nitrogen and stored at -80 °C until further processing. All samples used in this study were approved by the Committees for Ethical Review of Research Involving Human Subjects at Shandong Provincial Hospital.

Human HCC cell lines HepG2, MHCC-97H, Huh-7, Hep-3B and SMCC-7721, human normal liver cell line (LO2), human monocytic leukemia cell THP-1 were purchased from the Type Culture Collection of the Chinese Academy of Sciences (Shanghai, China). All these cell lines were cultured in Dulbecco's modified Eagle's medium (DMEM) or RIPM-1640 medium supplemented with 10% FBS (Gibco) at 37 °C.

The THP-1 and Huh-7 co-culture system were established to simulate the microenvironment of HCC as previously reported [22]. Briefly, THP-1 cells were seeded into 6-well plates and differentiated with 200 ng/mL PMA for 24 h [23]. Meanwhile, Huh-7 cells were transfected with expression vector for 24 h then seeded into transwell at a density of 1.5×10^5 cells per chamber. The differentiated THP-1 cells were washed three times with PBS and then co-cultured with Huh-7 cells for another 24 h. At the end of the treatment, THP-1 cells were harvested for FCM, RT-qPCR and western blot assay, the medium was collected for ELISA assay.

RNA immunoprecipitation (RIP)

RIP was conducted with a Magna RIP ^{TM} RNA-binding protein immunoprecipitation kit (Millipore, USA) according to the manufacturer's guidelines. Briefly, anti-Ago2 antibody and rabbit IgG was incubated with magnetic beads at room temperature for 30 min to generate antibody-coated beads. Approximately 1×10^7 cells were lysed and mixed at 4 °C overnight. After wash, co-immunoprecipitated RNA was extracted and detected using RT-qPCR.

Pull-down assay

Biotin-labelled hsa_circ_ 0110102 or oligo probes (GenePharma, China) were pre-incubated with Streptavidin-Dyna beads M-280 (#11206D, Invitrogen, USA) as described before [24]. hsa_circ_ 0110102 overexpressing and control cells were lysed and incubated with the beads at 4 °C overnight. Then, RNA was extracted and measured by RT-qPCR.

Florescence in situ hybridization (FISH)

Huh-7 cells were seeded into confocal dishes and fixed with 4% paraformaldehyde overnight. Cy3-labelled hsa_circ_0110102 probe (5'-GGTGCAATCGGACACCTTGGATATTGCAGACA-3'-Cy3) was designed and synthesized by GenePharma (Shanghai, China). Nuclei were counterstained with 4,6-diamidino-2-phenylindole (DAPI). All processes were conducted according to the manufacturer's instructions. Images were obtained by a FV3000 microscope (Olympus, Japan).

Western blot analysis

Cells were homogenized in ice-cold lysis buffer as described before [25]. The protein in cytoplasm and nucleus protein were extracted by kit from Beyotime (Shanghai, China), then separated by SDS-PAGE and transfected onto PVDF membrane, immunoblotted with indicated primary antibodies and HRP-linked antibodies (1:5000 dilution; Anti-Rabbit IgG, #7074; Anti-mouse IgG, #7076; CST) and visualized using Tanon-5200 Chemiluminescence Imager (Tanon, Shanghai, China) with ECL substrate (Millipore, CA, USA). primary antibodies used were as follows: CCL2 (1:1000 dilution; ab9669, Abcam), COX-2 (1:1000 dilution; ab15191, Abcam), FoxO1 (1:1000 dilution; ab39670, Abcam), ERK1/2 (1:1000 dilution; #4695, CST), Phospho-ERK1/2 (1:1000 dilution; #4370, CST), JNK (1:1000 dilution; #9252, CST), Phospho-JNK (1:1000 dilution; #9255, CST), P38 (1:1000 dilution; #8690, CST), Phospho-P38 (1:1000 dilution; #8632, CST) and β-actin (1:5000 dilution; #3700, CST).

Cell proliferation assay

A Cell counting Kit-8 (CCK-8, #HY-K0301, MCE, Shanghai, China) method was utilized to assess the proliferation of cells. Transfected cells were seeded into 96-well plates at a density of 5×10^3 cells per well and incubated at 37 °C for indicated time. 10 μL CCK-8 solution was added into each well and incubated for 2 h before detect, and then absorbance at 450 nm was measured using a microplate reader (Varioskan LUX, Thermo Fisher, USA).

For EdU staining assay, an Edu staining kit (iFluor 647, ab222421, Abcam) was used according to the manufacturer's protocol. In brief, cells were seeded into 6-well plates and transfected for 48 h. Then, cells were stained with EdU solution for 2 h and fixed with 4% paraformaldehyde and cultured with 0.5% Triton X-100 for 10 min. Finally, cells were stained with DAPI for 10 min. Images were collected with a FV3000 microscope (Olympus, Japan).

Quantitative reverse-transcription PCR (RT-qPCR)

Total RNA was extracted using TRIzol reagent (#15596-026, Invitrogen), nuclear and cytoplasmic RNA was extracted with the PARIS™ Kit (#AM1921, Thermo Fisher) as previously reported [13]. RT-qPCR kits were purchased from TaKaRa Bio Inc (Dalian, China) and cDNA was synthesized according to the manufacturer's instruction. The Quant Studio 5 Real-Time PCR System (Applied Biosystems, USA) and the SYBR Green (no. B21202, Bimake, Houston, USA) were used for RT-qPCR assay. The expression levels of mRNA were normalized to GAPDH mRNA. Primers were purchased from Genscript biotech co., ltd. For miRNA assay, miRNA-specific Taqman PCR primers were obtained from Life Technologies (CA, USA).

Genes levels were normalized to U6 or GAPDH to generate $a2^{-\Delta\Delta Ct}$ value for the relative expression of each transcript. Primer sequences used in the experiments were as follows:

Gene	Forward (5′-3′)	Reverse (5′-3′)
hsa_circ_0110102	CCCAGGGAACCAATCTGTCC	GGTGAACTCCACAGCCACAT
ZNF562	CCCAGGGAACCAATCTGTCC	GGTGAACTCCACAGCCACAT
CCL2	GCTCATAGCAGCCACCTCATTC	CCGCCAAAATAACCGATGTGATAC
COX-2	CTGGCGCTCAGCCATACAG	CGCACTTATACTGGTCAAATCCC
GAPDH	GGAGCGAGATCCCTCCAAAAT	GGCTGTTGTCATACTTCTCATGG

Flow cytometry

The isolated TIL was incubated with CD68 and CCR2 antibody for 1 h at 4 °C; CCL2-stimulated PBMCs were incubated with CCR2 antibody for 1 h at 4 °C, then washed with PBS for three times and finally resuspended in 200 μL PBS and analyzed by flow cytometry.

For cell cycle analysis, HepG2 and Huh-7 cells were trypsinized and fixed with 70% ethanol overnight at 4°C, followed by staining with PI reagent. The percentage of cells in the G0/G1, S, and G2/M phases was recorded using Flow cytometry (BD Biosciences, NY, USA).The results obtained were analyzed by the software FlowJo.

ELISA assay

THP-1 cells were treated with 50 ng/ml rCCL2 or transfected with the expression vector, then cells were treated with or without 1 μM AS1842856 or infection with sh-FoxO1 for 24 h. The culture supernatant was collected, and were used to detect the concentration of VEGF (cat no. DVE00), COX-2 (cat no. AF4198), IL-6 (cat no. D6050) and PGE2 (cat no. KGE004B) secreted using ELISA kits (all from R&D, Minneapolis, MN, USA). The absorbance was measured at 450 nm using a microplate reader (Varioskan LUX, Thermo Fisher, USA).

In vitro migration and invasion assays

Cell migration and invasion were measured using Transwell assay as previously described [26].

Plasmid constructs and transfection

pSELECT-HA-mFoxO1-wild-type (Addgene plasmid # 83308) and Δ256 (Addgene plasmid # 83379) were a gift from Steven Abcouwer[27]. Full-length of CCL2 cDNA was amplified and cloned into a pcDNA3.1 expression vector. The CCL2 promoter sequence from positions -500 to + 1 and COX-2 promoter sequence from positions − 1,122 to + 27 relative to the transcriptional start site subcloned into pGL3-Basic vector, the point mutation in the FoxO1 binding site of COX-2 promoter was generated by site-directed mutagenesis that splices by overlapextension. FoxO1 shRNA and scrambled shRNA were purchased from

Obio technology Co., Ltd. (shanghai, China). Cells were seeded into 6-well plates for overnight culture, then transfected with hsa_circ_0110102 overexpression vector or siRNA, miR-NC, miR-580-5p mimic or inhibitor with lipofectamine 2000 for 48 h, blank vector-transfected cells were used as controls.

Chromatin immunoprecipitation assay

To detect the in vivo association of FoxO1 with human COX-2 promoter, chromatin immunoprecipitation (ChIP) analysis was performed as previously described using SimpleChIP Enzymatic Chromatin IP Kit (#9002, CST, USA) according to manufacturer's protocol [28]. ChIP-PCR was used for validation with the forward primer 5'-CACCGGGCTTACGCAATTTT-3' and the reverse primer 5'-ACGCTCACTGCAAGTCGTAT-3', which were specifically designed from the COX-2 promoter region (139 to + 29).

Luciferase assays

Cells were transfected with luciferase reporter plasmids and subsequently incubated for 24 h in the complete medium. Luciferase activity was measured using the Dual-luciferase reporter assay System (Promega, Madison, WI) and normalized to *Renilla* luciferase values. Measurements for three biological replicates were taken in triplicate and averaged.

Statistical analysis

Data are expressed as mean ± SEM. SPSS 21.0 was used for statistical analysis. Unpaired Student's t-test were used for comparation between two groups. Two-way ANOVA analysis using the Tukey test was employed to compare three groups or more. $P < 0.05$ was considered statistically significant.

Results

hsa_circ_0110102 is down-regulated in HCC cell lines and tissues

hsa_circ_0110102, with the 1252 bp spliced mature sequence length, is located at chr19: 9763628–9770143 and derived from exons 3 to 6 of the ZNF562 gene (Fig. 1A). We used the published GSE135806 data set to identify circRNAs differentially expressed between five HCC and five adjacent normal tissues from HBV-related male HCC patients, aged 43–57 [29], and found that, compared with the control tissues, the expression of hsa_circ_0110102 was down-regulated in HCC tissues (Fig. 1B). Compared with matched normal control tissues, hsa_circ_0110102 was low-expressed in 17 HCC tissues collected from our hospital (Fig. 1C). In the HCC cell lines (Hep3B, MHCC-97H, Huh-7, HepG2 and SMCC-7721), the expression of hsa_circ_0110102 was significantly lower than human normal LO2 hepatocytes (Fig. 1D). As Huh-7 and HepG2 showed the lower hsa_circ_0110102 levels than other HCC cells, we would use these two cell lines in the next studies to reveal the tumor suppressive effect in HCC.

hsa_circ_0110102 knockdown promotes HCC cell growth, migration and invasiveness

Next, we examined the relative abundance of hsa_circ_0110102 in the nucleus and cytoplasm of Huh-7 and HepG2 cells via nuclear mass separation assays (Fig. 2A) and FISH (Fig. 2B), concluded that hsa_circ_0110102 was mainly located in the cytoplasm.

To analyze the role of has_circ_0110102 in HCC, has_circ_0110102-specific small interfering RNAs (siRNAs) were used to down-regulate the expression levels of has_circ_0110102. Thus, siRNAs targeting the backsplice junction sequence of has_circ_0110102 and the full length of ZNF562 were designed. We found that siRNA targeting the backsplice junction knocked down only the circular transcript and did not affect the expression of linear species. Contrarily, siRNA targeting linear transcript knocked down only the ZNF562 linear transcript but not the circular transcript (Fig. S1). Huh-7 and HepG2 cells were transfected with hsa_circ_0110102 expression vector and siRNA then followed with CCK-8 assay, migration and invasion assay and found that compared with control cells, hsa_circ_0110102 knockdown dramatically induced the proliferation, cell migration and invasiveness, which were inhibited by the hsa_circ_0110102 overexpression (Fig. 2C-2E).

hsa_circ_0110102 acts as a sponge for miR-580-5p

The target miRNAs of hsa_circ_0110102 were predicted by the https://circinteractome.nia.nih.gov/. Seven candidate miRNAs (miR-338-3p, miR-766, miR-659, miR-580-5p, miR-595, miR-188-3p and miR-607) were chosen for the next study according to their higher context score percentile (Fig. S2 and Fig. 3A). The biotin labelled hsa_circ_0110102 probe robustly enriched hsa_circ_0110102 compared with the oligo probe in HCC cells, verifying the efficiency of the pull-down assay (Fig. 3B). RNA extracted from the pull-down assay was analyzed using RT-qPCR and found that hsa_circ_0110102 probe enriched most miR-580-5p than other miRNAs both in Huh-7 and HepG2 cells (Fig. 3C). The following luciferase reporter assay results showed that miR-580-5p mimics remarkably reduced the luciferase activity of hsa_circ_0110102, while, miR-580-5p overexpressed shows no effect on the activity of a LUC-circ_0110102-mutant reporter gene (Fig. 3D and 3E). Next, Anti-AGO2 RIP assay found that miR-580-5p mimics pulled down hsa_circ_0110102 through anti-AGO2 antibody not control IgG (Fig. 3F). Overall, our results demonstrated that hsa_circ_0110102 functions as a sponge for miR-580-5p.

miR-580-5p in HCC is associated with poor prognosis

By analyzing the TCGA database (http://ualcan.path.uab.edu/analysis-mir.html), we found that miR-580-5p expression was increased in HCC tissues (Fig. 4A), and the KM-plotter (http://kmplot.com/analysis/) database also showed that miR-580-5p was associated with the lower survival rate in 372 HCC patients (Fig. 4B). The higher expressions of miR-580-5p were observed in five HCC cell lines (Fig. 4C).

Next, we investigated the effect of miR-580-5p on cell proliferation in HCC. Transfected with miR-580-5p inhibitor significantly decreased the miR-580-5p expression in Huh-7 and HepG2 cells (Fig. 4D). CCK-8 assay indicated that miR-580-5p inhibitor also inhibited cell proliferation rate (Fig. 4E), which was confirmed with EdU staining assay to detect DNA synthesis levels (Fig. 4F and 4G), cell cycle analyze

showed that less cells were in S phase after miR-580-5p inhibitor transfection (Fig. 4H). These results indicating for the first time that miR-580-5p may function as an oncogene in the development of HCC.

CCL2 is a direct target of miR-580-5p

By searching on Miranda (http://www.microrna.org/) and Targetscan (http://www.targetscan.org/), we found that there exists binding site between miR-580-5p and the 3'-UTR of CCL2 (Fig. 5A). Overexpression of miR-580-5p increased the mRNA and protein levels of CCL2 both in Huh-7 and HepG2 cells and the content of CCL2 in the culture medium, indicating that miR-580-5p overexpression increased the synthesis and secretion of CCL2 in HCC cells. But co-transfected with hsa_circ_0110102 significantly down-regulated the CCL2 mRNA, protein and the concentration in the medium (Fig. 5B & 5C), indicating that hsa_circ_0110102 functions as a miR-580-5p sponge to inhibit the expression of CCL2.

We then constructed pGL3 plasmids containing the CCL2 3'-UTR wile type and mutant sequence. Compared with the NC group, the miR-580-5p overexpression showed a significant increase in relative Rluc activity in both Huh-7 and HepG2 cells, hsa_circ_0110102 showed no effect on the CCL2 promoter activation. However, co-transfection with hsa_circ_0110102 abolished the effect. However, mutating the CCL2 3'-UTR binding site blocked the effect of miR-580-5p and hsa_circ_0110102 (Fig. 5D). The CCL2 mRNA and protein levels were detected with RT-qPCR and western blotting, the results showed that, miR-580-5p mimic significantly. We then used miR-580-5p inhibitor and siRNA targeting hsa_circ_0110102 to examine whether hsa_circ_0110102 inhibit the CCL2 expression levels in HCC cell by antagonist the miR-580-5p effect. The results showed that si-hsa_circ_0110102 could abolish the miR-580-5p inhibitor-induced downregulation of CCL2 mRNA and protein expression levels (Fig. 5E and 5F). miR-580-5p overexpression increased the migration and invasion of Huh-7 cells, hsa_circ_0110102 significantly inhibited the effect of miR-580-5p (Fig. 5G). These results showed that, CCL2 is identified to be a direct target of miR-580-5p, and hsa_circ_0110102 act as a sponge for miR-580-5p to block the CCL2 induce effect.

AS1842856 inhibits CCL2 induced CCR2 expression and cytokine secretion in macrophages

Previously studies found that, CCL2 secreted from hepatocytes triggers macrophage recruitment and could induce liver fibrosis, and even HCC [30]. In tumor microenvironment, CCL2 interacts with CCR2, which on the surface of macrophage, to mediate chemotaxis of monocytes and TAM to facilitates cancer progression [15]. Our results have shown that, hsa_circ_0110102 act as a sponge for miR-580-5p and inhibited the CCL2 expression and secretion from HCC cells. Next, we use the THP-1 and Huh-7 co-culture system to detect their effect on the macrophage phenotype and function. The FCM results showed that $CD68^+$ macrophages cell developed polarized CCR2 phenotypes in THP-1, and that the percentage of $CCR2^+CD68^+$ cells increased significantly in the miR-580-5p mimic group, but co-transfection with hsa_circ_0110102 blocked the effect of miR-580-5p (Fig. 6A).

Previous studies have shown that COX-2 and PGE2 in the tumor microenvironment which released from macrophage was critical in the HCC development. As shown in Fig. 6B and 6C, miR-580-5p significantly induced the COX-2 mRNA and protein expression in THP-1 cells and increased the content of COX-2 in the co-culture medium. As COX-2 is a rate-limiting enzyme in regulating PGE2-generation and its expression is highly inducible in macrophages[31]. PGE2, which induces the secretion of vascular endothelial growth factor (VEGF) to accelerate neovascularization in HCC [32]. We also found that, miR-580-5p induced and hsa_circ_0110102 blocked the PGE2 expression in the co-culture system (Fig. 6D).

Previously studies found that, FoxO1 could promote pro-inflammation cytokine release of macrophage [33]. The activation of FoxO1 was also involved in the regulation of COX-2 expression [34, 35]. So, we suspected whether CCL2-induced COX-2 expression increasement was mediated through FoxO1 dependent manner in macrophage. As shown in Fig. S3, Fig. 6E and 6F, 50 ng/ml rCCL2 significantly up-regulated the mRNA and protein levels of COX-2 in THP-1 cells, and also the released COX-2, PGE2, VEGF and IL-6 in the medium, either FoxO1 knockdown or inhibitor AS1842856 significantly inhibited the effect of rCCL2, instead of blocked it. These results showed that CCL2 induce the COX-2/PGE2 pathway partly through FoxO1.

CCL2 induces FoxO1 activation via p38 MAPK pathway in THP-1 cells

Previous studies found that, MAPK pathway can active FoxO family [36]. Interestingly, autocrine CCL2 is associated with activation MAPK pathway [37]. We next investigated the relationship between MAPK pathway and FoxO1 activity in response to rCCL2 stimulation in macrophage. ChIP assay found that, rCCL2 stimulation significantly promoted the binding of FoxO1 on COX-2 promoter in a time-dependent manner in THP-1 cells (Fig. 7A), which was reversed by p38 inhibitor SB203580, while the JNK inhibitor SP600125 and ERK1/2 inhibitor SCH772984 shows no effect on the COX-2 promoter activity (Fig. 7B). These results demonstrate that CCL2 induced FoxO1 activation via p38 MAPK.

Using luciferase assay, we found that, both rCCL2 or forced overexpression of CCL2 increased COX-2 promoter transcription activity, FoxO1 co-operate with CCL2 caused a more significant increase, while pretreated with AS1842856 inhibited the transcription level (Fig. 7C). FoxO1-Δ256, lacking the transactivation domain of FoxO1, was used to detect whether this site function in the regulation COX-2 activity. THP-1 cells were co-transfected with FoxO1 WT and Δ256 expression vectors, via luciferase assay, we found that WT enhanced COX-2 transcription activity, but no similar enhancement was observed in Δ256 mut. AS1842856 and p38 MAPK inhibitors treatment both decreased the COX-2 transcription activity, but ERK and JNK inhibitor shows no effect (Fig. 7D). Implying that, in the physiologic state, Δ256 site of FoxO1 was quite important for the transcript activation effect of COX-2.

Next, a COX-2 promoter upstream region mutation was subcloned into pGL3-Basic to define FoxO1 target site on the COX-2 promoter, after co-transfection with FoxO1 into THP-1 cells, the activity of promoter variants was determined. As shown in Fig. 7E, the activity of promoter variants with DNA deletions up to − 111 nt and − 101 nt shows no difference in the presence or absence of FoxO1, but FoxO1 significantly

induced the WT promoter activity. These results indicating that, the FoxO1 target site was localized to the − 111/−101-nt region of the COX-2 promoter.

Discussion

CircRNAs are endogenous noncoding RNAs that been regarded as potential novel diagnostic and prognostic molecular biomarkers in cancer [38]. Recently, mounting evidence have identified the important roles of circRNAs in the carcinogenesis and development of HCC, but little focus on its functional role in regulating the crosstalk between cancer cells and microenvironment. Microenvironment composed of fibroblasts, endothelial cells and immune system cells, that interact with tumor mass could promote the progression of cancer [39, 40]. Among them, macrophages account for a large proportion in tumors, and also called TAM. Notably, TAM acts directly on tumor cells and acts indirectly on the tumor microenvironment through cytokines, like VEGF and IL-6, which enhancing cancer cell invasion and metastasis, angiogenesis ability [41].

Macrophages participate in the inflammatory environment of mutagenesis in the early stage of tumor development, and as the tumor progresses to malignant, it also can stimulate angiogenesis and promote tumor migration, invasion and inhibition of tumor immunity [42]. Many clinical studies have shown that macrophages may promote tumorigenesis. CircRNAs have also shown potential effect to influence the tumor microenvironment, Circular RNA CDR1as may play a specific role in immune and stromal cell infiltration in tumor tissue, especially those of $CD8^+$ T cells, activated NK cells, M2 macrophages [43]. Circular RNA CircASAP1 could mediates tumor-associated-macrophage infiltration by regulating the miR-326/miR-532-5p-CSF-1 pathway [14]. So, targeting circular RNA on the tumor microenvironment may be a potential direction in the future.

This study focused on the hsa_circ_0110102 to discover novel HCC therapy targets. Our research found that hsa_circ_0110102 was down-regulated in HCC tissues and knockdown of hsa_circ_0110102 inhibits cell proliferation, invasion and migration *in vitro*. As circular RNAs may act as sponge of miRNA to regulate the target gene function, we use luciferase reporter assays and bioinformatics prediction revealed that hsa_circ_0110102 may compete for binding with miR-580-5p.

Aberrant miR-580-5p expressions in many tumor has been investigated, like glioma and breast cancer[44, 45], but until now, it's exactly mechanistic contribution to HCC progression has not been explored. Our study indicated that, miR-580-5p levels in tumor tissues were dramatically higher than that of the adjacent normal tissue, and miR-580-5p could promotes the proliferation, invasion and migration of HCC. We further confirmed that hsa_circ_0110102 act as an endogenous sponge on miR-580-5p to regulates the expression of CCL2.

CCL2 as a chemokine, bind to CCR2 and chemotactic for monocytes and macrophages, is an important human CC chemokine which shows a strong tendency to monocytes. It plays an important role in physiopathological reactions such as inflammation, pathogen infection, and tumor formation [46]. Many

research has shown that, CCL2 is closely related to tumorigenesis and related to the poor prognosis in various cancers such as HCC [47], lung cancer, breast cancer [48] and prostate cancer [49]. Blocking the CCL2-CCR2 signaling pathway can inhibit malignant tumor growth, metastasis, reduce postoperative recurrence, and improve survival [50].

A growing number of cellular signaling pathways have been implicated in orchestrating the process of COX-2/PGE2 pathway in tumor development. COX-2 acts as the rate-limiting enzyme of PGE2, is considered to be an important mediator in inflammatory responses and is highly expressed in a variety of tumors. It interacts with many cytokines and other members of the prostaglandin family to constitute a complex network system. Several studies suggest that high levels of PGE2 are also involved in the inflammatory response and plays a predominant role in promoting tumor growth and is associated with poor prognosis. Moreover, *in vivo* studies have further indicated that the specific inhibition of COX-2 shows a protective effect on HCC development and slow down the tumor progression in mouse models [51].

FoxO1, an important transcription factor which has been shown to be involved in various cellular functions, activated in response to a wide range of external stimuli, like growth factors, insulin and oxidative stress [52]. Recently, FoxO1 activation have been shown to participate in COX-2/PGE2-dependent cell migration [53]. To comprehensively understand the effect of CCL2 on macrophage, we performed *in vitro* assays to testify the effect of transcription factor FoxO1 on CCL2 induced COX-2/PGE2 pathway activation, our results showed that FoxO1 knockdown and inhibitor decreases the COX-2 and PGE2 expression and inhibits the migration and tube formation. To further explore the role of FoxO1 pathway in the regulation of COX-2/PGE2 pathway in macrophage, ChIP assay was used to investigate the binding effect of FoxO1 on COX-2 promoter, luciferase assay was obtained to analyze the inhibition effect of CCL2 on COX-2 promoter transcription activity. FoxO1 WT were used to active the endogenous activity and Δ256 mut-FoxO1, a loss of function FoxO1 mutation, was used as a negative control. As we expected, FoxO1 increased the COX-2 transcription activity, but Δ256 mut-FoxO1 showed no similar effect. We further detected the binding site of FoxO1 on COX-2 promoter using a point mutation promoter luciferase vector.

Conclusions

Taken together, our data indicated that, hsa_circ_0110102 shows critical regulatory role as an oncogenic circRNA through the sponge effect of miR-580-5p to inhibit the expression of CCL2 in HCC cells. CCL2 could further actives COX-2/PGE2 pathway in macrophage via FoxO1-dependent manner (Fig. 8). Overall, the present research throw light on targeting the hsa_circ_00110102/miR-580-5p/CCL2 axis may be a promising therapeutic strategy for HCC.

Declarations

Notes

Xinxing Wang and Wei Sheng contributed equally to this work.

Acknowledgement

This work was supported by the National Natural Science Foundation of China (No. 81870205) and the Natural Science Foundation of Shandong Province, China (No. ZR2012HM -079).

Competing interests

The authors declare that they have no competing interests.

Availability of data and materials

All the data is contained in the manuscript.

Consent for publication

Not applicable.

Ethics approval and consent to participate

A total of 17 patients with hepatocellular carcinoma were enrolled at Shandong Provincial Hospital Affiliated to Shandong First Medical University (Jinan, Shandong, China). Our study was approved by the Ethics Committee of Shandong Provincial Hospital (Registration number: SS-2017-093). Written informed consent was obtained from all patients.

Author contributions

Conceptualization, Z.Z., R.G. and Y.W.; methodology, X.W. and W.S.; software, D.D.; validation, Z.W. and D.D.; formal analysis, X.W. and T.X; investigation, X.W., T.X., and J.X..; resources, J.C. and Z.R.; data curation, Z.W.; writing—original draft preparation, X.W. and W.S.; writing—review and editing, R.G. and Z.Z.; visualization, J.X.; supervision, Z.Z. and R.G.; project administration, Z.Z.; funding acquisition, Z.Z. and R.G.. All authors have read and agreed to the published version of the manuscript.

Funding

This work was supported by the National Natural Science Foundation of China (No. 81870205) and the Natural Science Foundation of Shandong Province, China (No. ZR2012HM -079).

Data availability

The data used to support the findings in this study are available upon reasonable request from the corresponding authors.

Abbreviations

HCC hepatocellular carcinoma

UTR untranslated coding regions

CCL2 C-C motif chemokine ligand 2

CCR C-C motif chemokine receptor

COX-2 cyclooxygenase-2

PGE2 prostaglandin E2

FoxO1 forkhead box O1

ceRNA competing endogenous RNA

TAM tumor-associated macrophages

ZNF562 zinc finger protein 562

CCK-8 cell counting kit-8

FISH fluorescence in situ hybridization

CHIP chromatin Immunoprecipitation

GAPDH glyceraldehyde-3-phosphate dehydrogenase

PCR polymerase chain reaction

References

1. Jemal A, Bray F, Center MM, Ferlay J, Ward E, Forman D. Global cancer statistics. Cancer J Clin. 2011;61:69–90.
2. Bray F, Ferlay J, Soerjomataram I, Siegel RL, Torre LA, Jemal A. Global cancer statistics 2018: Globocan estimates of incidence and mortality worldwide for 36 cancers in 185 countries. Cancer J Clin. 2018;68:394–424.
3. Anastasiadou E, Jacob LS, Slack FJ. Non-coding rna networks in cancer. Nature reviews Cancer. 2018;18:5–18.
4. Salzman J. Circular rna expression: Its potential regulation and function. Trends Genet. 2016;32:309–16.
5. Kristensen LS, Hansen TB, Veno MT, Kjems J. Circular rnas in cancer: Opportunities and challenges in the field. Oncogene. 2018;37:555–65.

6. Bei Y, Yang T, Wang L, Holvoet P, Das S, Sluijter JPG, Monteiro MC, Liu Y, Zhou Q, Xiao J. Circular rnas as potential theranostics in the cardiovascular system. Molecular therapy Nucleic acids. 2018;13:407–18.
7. Xu Z, Li P, Fan L, Wu M. The potential role of circrna in tumor immunity regulation and immunotherapy. Frontiers in immunology. 2018;9:9.
8. Zhang L. Circular rna: The main regulator of energy metabolic reprogramming in cancer cells. Thoracic cancer. 2020;11:6–7.
9. Xu S, Zhou L, Ponnusamy M, Zhang L, Dong Y, Zhang Y, Wang Q, Liu J, Wang K. A comprehensive review of circrna: From purification and identification to disease marker potential. PeerJ. 2018;6:e5503.
10. Cao L, Wang M, Dong Y, Xu B, Chen J, Ding Y, Qiu S, Li L, Karamfilova Zaharieva E, Zhou X, Xu Y. Circular rna circrnf20 promotes breast cancer tumorigenesis and warburg effect through mir-487a/hif-1alpha/hk2. Cell Death Dis. 2020;11:145.
11. Taborda MI, Ramirez S, Bernal G. Circular rnas in colorectal cancer: Possible roles in regulation of cancer cells. World J Gastrointest Oncol. 2017;9:62–9.
12. Fischer JW, Leung AK. Circrnas: A regulator of cellular stress. Crit Rev Biochem Mol Biol. 2017;52:220–33.
13. Liu B, Yang G, Wang X, Liu J, Lu Z, Wang Q, Xu B, Liu Z, Li J. Circbach1 (hsa_circ_0061395) promotes hepatocellular carcinoma growth by regulating p27 repression via hur. J Cell Physiol 2020.
14. Hu ZQ, Zhou SL, Li J, Zhou ZJ, Wang PC, Xin HY, Mao L, Luo CB, Yu SY, Huang XW, Cao Y, Jia F, Zhou J. Circular rna sequencing identifies circasap1 as a key regulator in hepatocellular carcinoma metastasis. Hepatology 2019.
15. Qian BZ, Li J, Zhang H, Kitamura T, Zhang J, Campion LR, Kaiser EA, Snyder LA, Pollard JW. Ccl2 recruits inflammatory monocytes to facilitate breast-tumour metastasis. Nature. 2011;475:222–5.
16. Teng KY, Han J, Zhang X, Hsu SH, He S, Wani NA, Barajas JM, Snyder LA, Frankel WL, Caligiuri MA, Jacob ST, Yu J, Ghoshal K. Blocking the ccl2-ccr2 axis using ccl2-neutralizing antibody is an effective therapy for hepatocellular cancer in a mouse model. Mol Cancer Ther. 2017;16:312–22.
17. Lin A, Wang G, Zhao H, Zhang Y, Han Q, Zhang C, Tian Z, Zhang J. Tlr4 signaling promotes a cox-2/pge2/stat3 positive feedback loop in hepatocellular carcinoma (hcc) cells. Oncoimmunology. 2016;5:e1074376.
18. Carvalho MI, Pires I, Prada J, Raposo TP, Gregório H, Lobo L, Queiroga FL. High cox-2 expression is associated with increased angiogenesis, proliferation and tumoural inflammatory infiltrate in canine malignant mammary tumours: A multivariate survival study. Veterinary Comparative Oncology. 2017;15:619.
19. Lu Y, Shi C, Qiu S, Fan Z. Identification and validation of cox-2 as a co-target for overcoming cetuximab resistance in colorectal cancer cells. Oncotarget. 2016;7:64766–77.
20. Regulski M, Regulska K, Prukała W, Piotrowska H, Stanisz B, Murias M. Cox-2 inhibitors: A novel strategy in the management of breast cancer. Drug Discovery Today. 2016;21:598–615.

21. Wang D, DuBois RN. The role of cox-2 in intestinal inflammation and colorectal cancer. Oncogene. 2009;29:781–8.
22. Wewering F, Jouy F, Wissenbach DK, Gebauer S, Bluher M, Gebhardt R, Pirow R, von Bergen M, Kalkhof S, Luch A, Zellmer S. Characterization of chemical-induced sterile inflammation in vitro: Application of the model compound ketoconazole in a human hepatic co-culture system. Arch Toxicol. 2017;91:799–810.
23. Shiratori H, Feinweber C, Luckhardt S, Linke B, Resch E, Geisslinger G, Weigert A, Parnham MJ. Thp-1 and human peripheral blood mononuclear cell-derived macrophages differ in their capacity to polarize in vitro. Mol Immunol. 2017;88:58–68.
24. Yan D, Dong W, He Q, Yang M, Huang L, Kong J, Qin H, Lin T, Huang J. Circular rna circpicalm sponges mir-1265 to inhibit bladder cancer metastasis and influence fak phosphorylation. EBioMedicine. 2019;48:316–31.
25. Yu D, Chen G, Pan M, Zhang J, He W, Liu Y, Nian X, Sheng L, Xu B. High fat diet-induced oxidative stress blocks hepatocyte nuclear factor 4 ± and leads to hepatic steatosis in mice. J Cell Physiol. 2017;233:4770–82.
26. Yang J, Lv X, Chen J, Xie C, Xia W, Jiang C, Zeng T, Ye Y, Ke L, Yu Y. Ccl2-ccr2 axis promotes metastasis of nasopharyngeal carcinoma by activating erk1/2-mmp2/9 pathway. Oncotarget. 2016;7:15632–47.
27. Kong D, Gong L, Arnold E, Shanmugam S, Fort PE, Gardner TW, Abcouwer SF. Insulin-like growth factor 1 rescues r28 retinal neurons from apoptotic death through erk-mediated bimel phosphorylation independent of akt. Exp Eye Res. 2016;151:82–95.
28. Hu H, Han T, Zhuo M, Wu LL, Yuan C, Wu L, Lei W, Jiao F, Wang LW. Elevated cox-2 expression promotes angiogenesis through egfr/p38-mapk/sp1-dependent signalling in pancreatic cancer. Sci Rep. 2017;7:470.
29. Yu J, Ding WB, Wang MC, Guo XG, Xu J, Xu QG, Yang Y, Sun SH, Liu JF, Qin LX, Liu H, Yang F, Zhou WP. Plasma circular rna panel to diagnose hepatitis b virus-related hepatocellular carcinoma: A large-scale, multicenter study. Int J Cancer. 2020;146:1754–63.
30. Filliol A, Schwabe RF: Foxm1 induces ccl2 secretion from hepatocytes triggering hepatic inflammation, injury, fibrosis, and liver cancer. Cellular and molecular gastroenterology and hepatology 2020.
31. Che D, Zhang S, Jing Z, Shang L, Jin S, Liu F, Shen J, Li Y, Hu J, Meng Q. Macrophages induce emt to promote invasion of lung cancer cells through the il-6-mediated cox-2/pge2/β-catenin signalling pathway. Mol Immunol. 2017;90:197–210.
32. Iñiguez MA, Rodríguez A, Volpert OV, Fresno M, Redondo JM. Cyclooxygenase-2: A therapeutic target in angiogenesis. Trends in Molecular Medicine. 2003;9:73–8.
33. Yang JB, Zhao ZB, Liu QZ, Hu TD, Long J, Yan K, Lian ZX. Foxo1 is a regulator of mhc-ii expression and anti-tumor effect of tumor-associated macrophages. Oncogene. 2018;37:1192–204.

34. Liu X, Cui Y, Li M, Xu H, Zuo J, Fang F, Chang Y. Cobalt protoporphyrin induces ho-1 expression mediated partially by foxo1 and reduces mitochondria-derived reactive oxygen species production. Plos One. 2013;8:e80521.
35. Chen G, Yu D, Xue N, Liu J, Koenig RJ, Xu B, Sheng L. Lncrna sra promotes hepatic steatosis through repressing the expression of adipose triglyceride lipase (atgl). Sci Rep. 2016;6:35531.
36. Asada S, Daitoku H, Matsuzaki H, Saito T, Sudo T, Mukai H, Iwashita S, Kako K, Kishi T, Kasuya Y, Fukamizu A. Mitogen-activated protein kinases, erk and p38, phosphorylate and regulate foxo1. Cell Signal. 2007;19:519–27.
37. Guo F, Xu D, Lin Y, Wang G, Wang F, Gao Q, Wei Q, Lei S. Chemokine ccl2 contributes to bbb disruption via the p38 mapk signaling pathway following acute intracerebral hemorrhage. FASEB journal: official publication of the Federation of American Societies for Experimental Biology. 2020;34:1872–84.
38. Zhao D, Liu H, Liu H, Zhang X, Zhang M, Kolluri VK, Feng X, He Z, Wang M, Zhu T, Yan X, Zhou Y. Downregulated expression of hsa_circ_0037515 and hsa_circ_0037516 as novel biomarkers for non-small cell lung cancer. Am J Transl Res. 2020;12:162–70.
39. Landskron G, De lFM, Thuwajit P, Thuwajit C, Hermoso MA. Chronic inflammation and cytokines in the tumor microenvironment. J Immunol Res. 2014;2014:149185.
40. Dehne N, Mora J, Namgaladze D, Weigert A, Brune B. Cancer cell and macrophage cross-talk in the tumor microenvironment. Curr Opin Pharmacol. 2017;35:12–9.
41. Kim J, Bae JS. Tumor-associated macrophages and neutrophils in tumor microenvironment. Mediat Inflamm. 2016;2016:6058147.
42. Qian BZ, Pollard JW. Macrophage diversity enhances tumor progression and metastasis. Cell. 2010;141:39–51.
43. Zou Y, Zheng S, Deng X, Yang A, Xie X, Tang H, Xie X. The role of circular rna cdr1as/cirs-7 in regulating tumor microenvironment: A pan-cancer analysis. Biomolecules 2019;9.
44. Almog N, Ma L, Schwager C, Brinkmann BG, Beheshti A, Vajkoczy P, Folkman J, Hlatky L, Abdollahi A. Consensus micro rnas governing the switch of dormant tumors to the fast-growing angiogenic phenotype. PLoS One. 2012;7:e44001.
45. Nairismagi ML, Vislovukh A, Meng Q, Kratassiouk G, Beldiman C, Petretich M, Groisman R, Fuchtbauer EM, Harel-Bellan A, Groisman I. Translational control of twist1 expression in mcf-10a cell lines recapitulating breast cancer progression. Oncogene. 2012;31:4960–6.
46. Fridlender ZG, George B, Veena K, Guanjun C, Jing S, Sunil S, Cecilia M, Cecilia C, Wang C, Daniel LCS. H: Ccl2 blockade augments cancer immunotherapy. Can Res. 2010;70:109.
47. Li X, Yao W, Yuan Y, Chen P, Li B, Li J, Chu R, Song H, Xie D, Jiang X. Targeting of tumour-infiltrating macrophages via ccl2/ccr2 signalling as a therapeutic strategy against hepatocellular carcinoma. Gut. 2015;66:157.
48. BZ Q, H JL, LR ZTKJZ, EA C, LA K, JW S. P: Ccl2 recruits inflammatory monocytes to facilitate breast-tumour metastasis. Nature. 2012;475:222–5.

49. Loberg RD, Day LSL, Jason H, Chi Y, John LN, St, Ryan G, Neeley CK, Pienta KJ. Ccl2 is a potent regulator of prostate cancer cell migration and proliferation. Neoplasia. 2006;8:578–86.
50. Roblek M, Strutzmann E, Zankl C, Adage T, Heikenwalder M, Atlic A, Weis R, Kungl A, Borsig L. Targeting of ccl2-ccr2-glycosaminoglycan axis using a ccl2 decoy protein attenuates metastasis through inhibition of tumor cell seeding 1. Neoplasia. 2016;18:49–59.
51. Gungor H, Ilhan N, Eroksuz H. The effectiveness of cyclooxygenase-2 inhibitors and evaluation of angiogenesis in the model of experimental colorectal cancer. Biomed Pharmacother. 2018;102:221–9.
52. Tikhanovich I, Cox J, Weinman SA. Forkhead box class o transcription factors in liver function and disease. J Gastroenterol Hepatol. 2013;28(Suppl 1):125–31.
53. Hsu CK, Lin CC, Hsiao LD, Yang CM. Mevastatin ameliorates sphingosine 1-phosphate-induced cox-2/pge2-dependent cell migration via foxo1 and creb phosphorylation and translocation. Br J Pharmacol. 2016;172:5360–76.

Figures

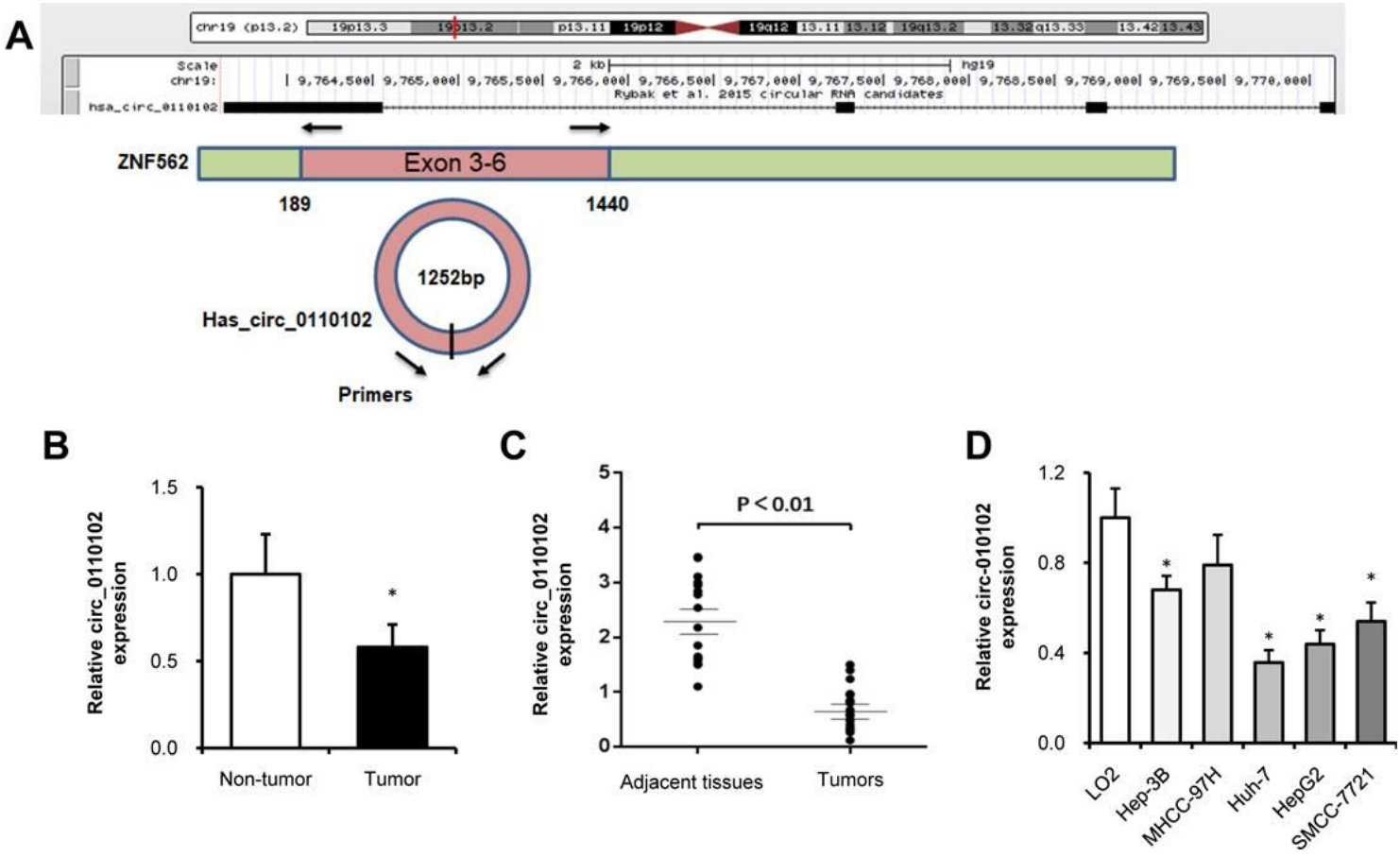

Figure 1

hsa_circ_0110102 was down-regulated in HCC tumor tissues and cell lines. (A) The genomic loci of hsa_circ_0110102, and the schematic model of the primers of hsa_circ_0110102. The primers target the

back-splice junction of hsa_circ_0110102. (B) The relative expression of hsa_circ_0110102 was validated in 5 pairs of normal and HCC tissues from GSE135806 dataset. (C) The expression of hsa_circ_0110102 mRNA was analyzed in 17 tumor tissues and 17 non-tumor tissues by RT-qPCR. (D) hsa_circ_0110102 expression levels in five HCC cell lines and LO2 cell were examined by RT-PCR. Data are presented as the mean ± S.E., *, P<0.05.

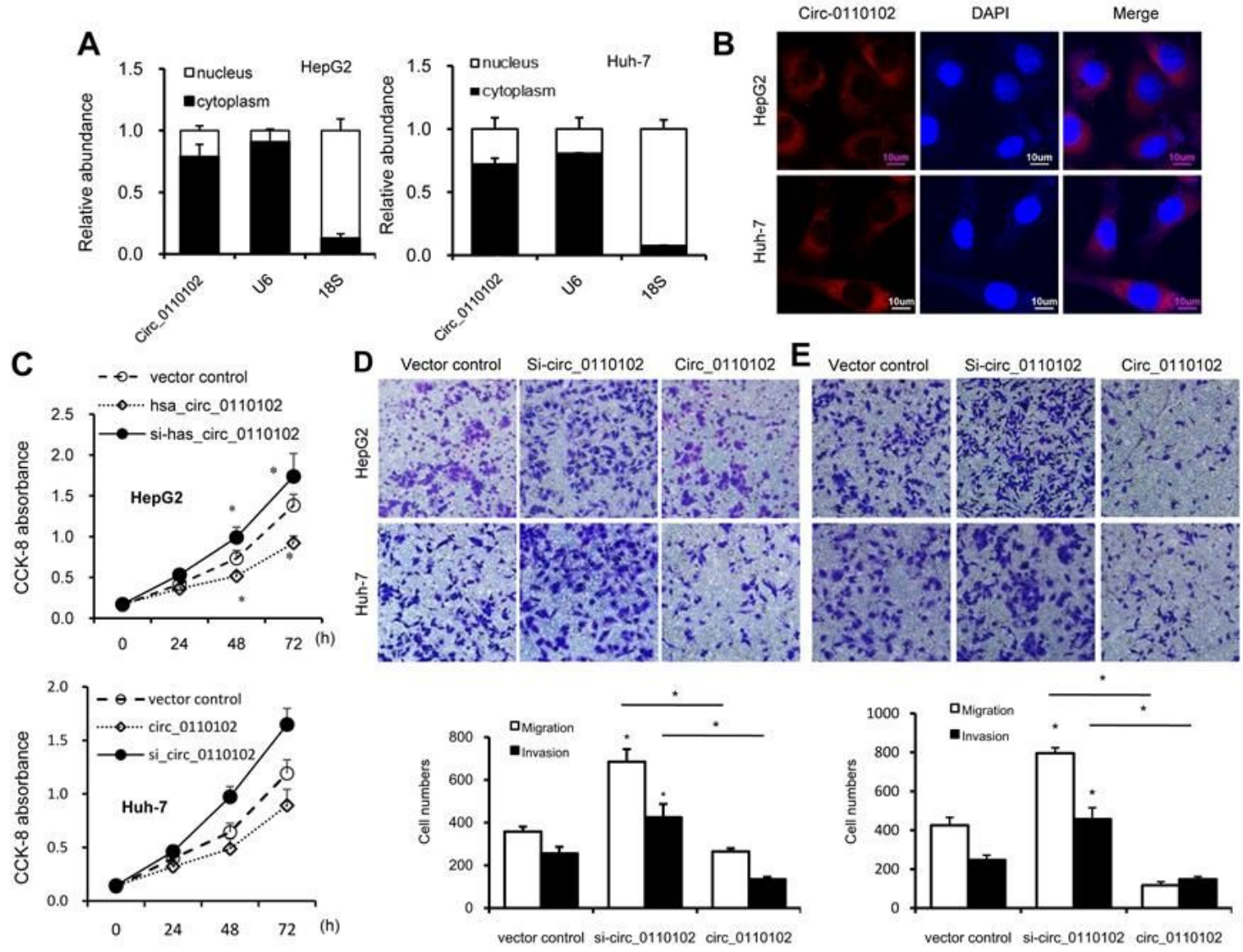

Figure 2

hsa_circ_0110102 inhibits the proliferation and migration ability of HCC in vitro. (A) The relative quantity of hsa_circ_0110102, U6 and 18S in the cytoplasmic and nuclear fractions of HCC cells was determined by RT-qPCR. (B) Subcellular localization of hsa_circ_0110102 was determined by FISH assay. (C) CCK-8 assays were performed to assess the proliferation of Huh-7 and HepG2 cells after transfection. (D-E) The ability of cell migration and invasion was measured by transwell assay in HCC tumor cell lines HepG2 and Huh-7 with si-circ_0110102 and circ_0110102 transfection. The representative magnified sections of transwell cell staining images are shown. Statistical results based on three independent experiments is shown in right. (200×). Data are presented as the mean ± S.E., *, P<0.05.

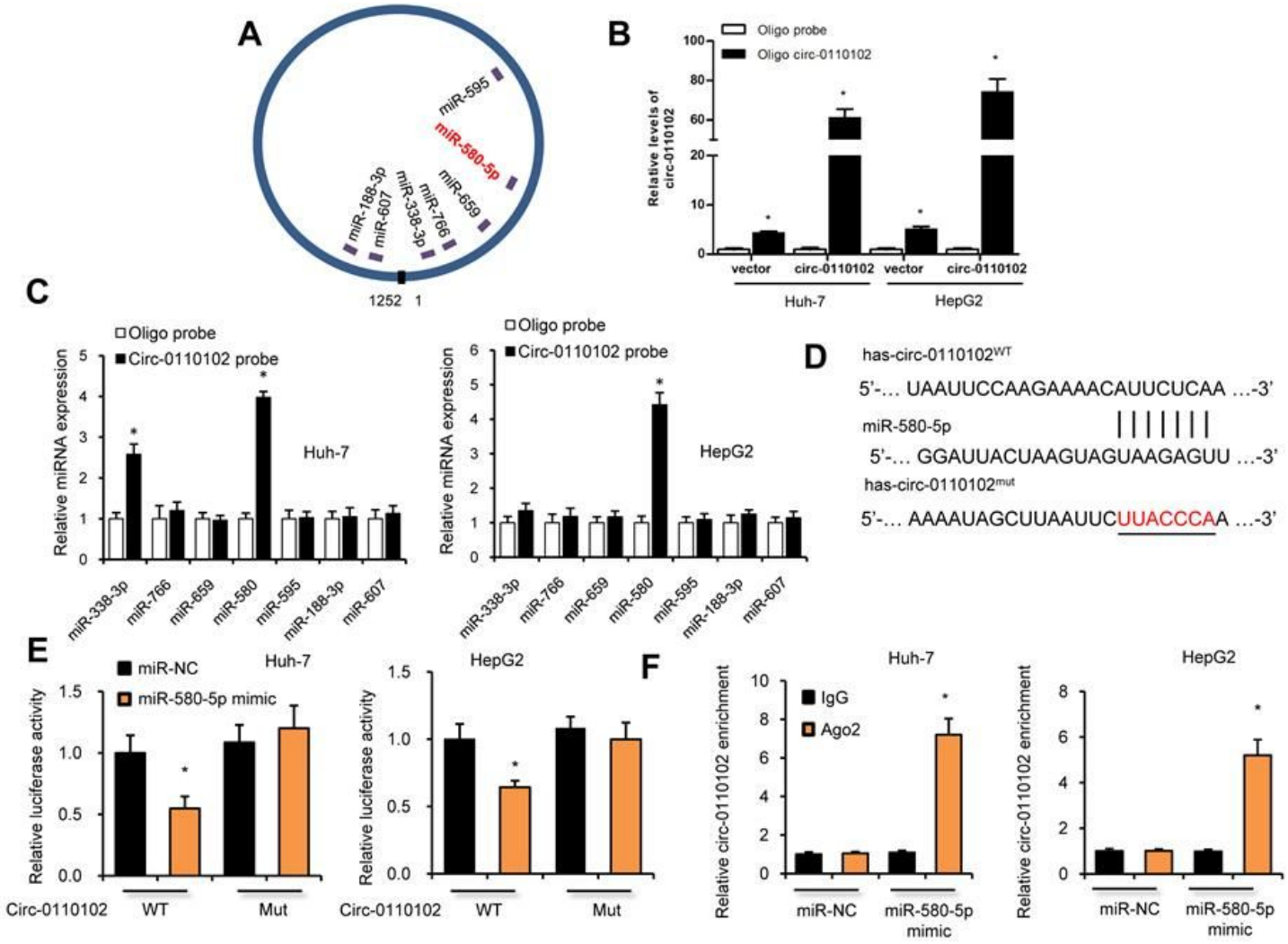

Figure 3

hsa_circ_0110102 served as a sponge for the miR-580-5p. (A) Schematic illustration of the predicted binding sites between hsa_circ_0110102 and seven candidate miRNAs. (B) RNA pull-down assay with hsa_circ_0110102 or oligo probes. (C) Relative levels of seven miRNAs in cell lysate pulled down by oligo or hsa_circ_0110102 probes were detected by RT-qPCR. (D) The predicted binding sites of miR-580-5p on hsa_circ_0110102. (E) Relative luciferase activity in Huh-7 and HepG2 cells after transfection of hsa_circ_0110102 Wt/Mut and the 3'-UTR of miR-580-5p. (F) Anti-AGO2 RIP was performed in Huh-7 and HepG2 cells after miR-580-5p NC or mimics transfection. Data are presented as the mean ± S.E., *, $P<0.05$.

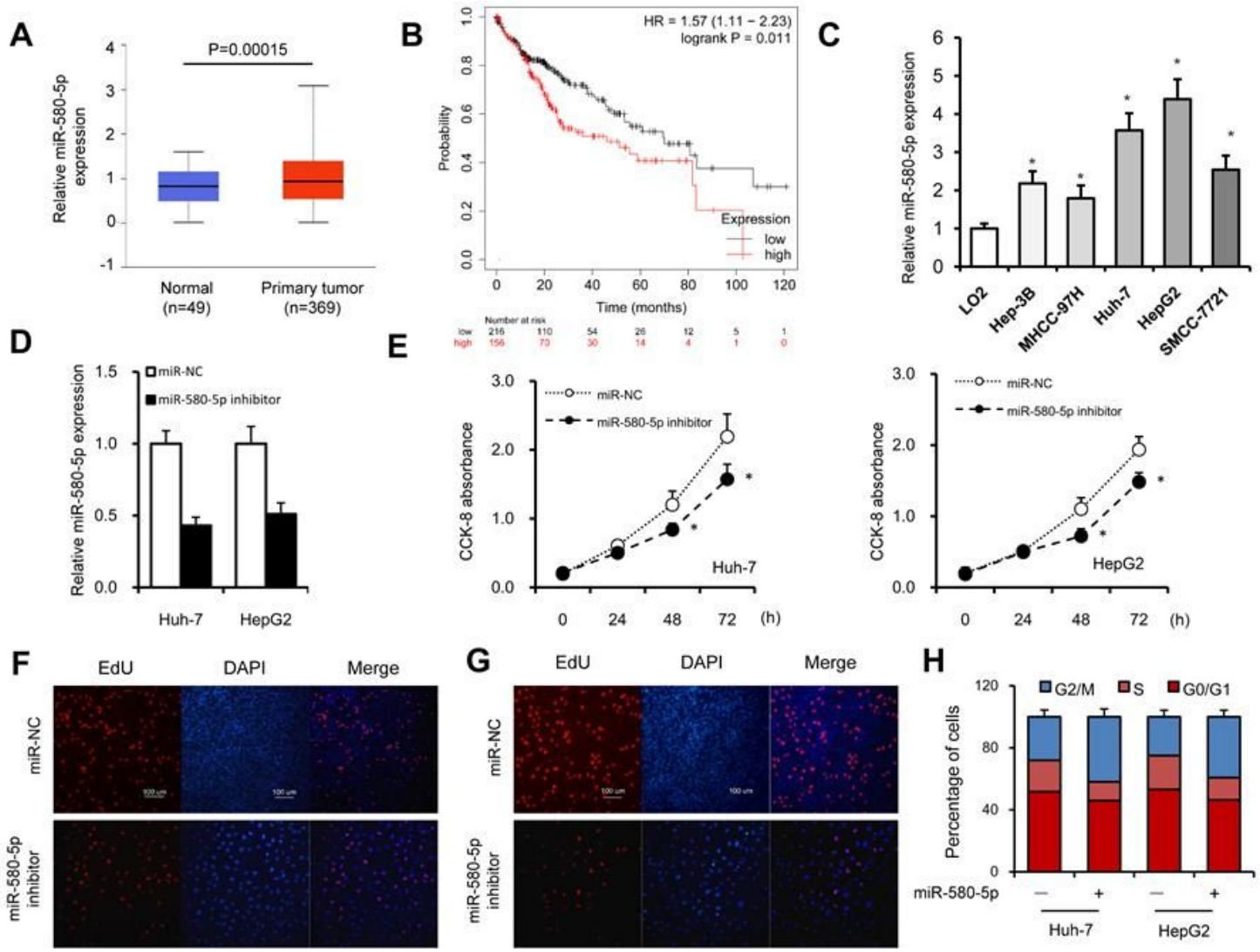

Figure 4

miR-580-5p was overexpressed in HCC tumor tissues and cell lines. (A) miR-580-5p levels in 49 normal and 369 primary HCC tissues. (B) Kaplan–Meier survival curve of patients in low and high miR-580-5p expression groups. (C) miR-580-5p levels in five HCC cell lines and LO2 cell were examined by RT-PCR. Huh-7 and HepG2 cells were transfected with miR-580-5p NC or mimic for 48 h. (D) The miR-580-5p levels were examined with RT-qPCR. (E) Cell viability was detected by CCK-8 assay. (F-G) EdU assays were used to detect the DNA synthesis in Huh-7 and HepG2 cells. (H) Cell cycle was detected with flow cytometry assays. Data are presented as the mean ± S.E., *, P<0.05.

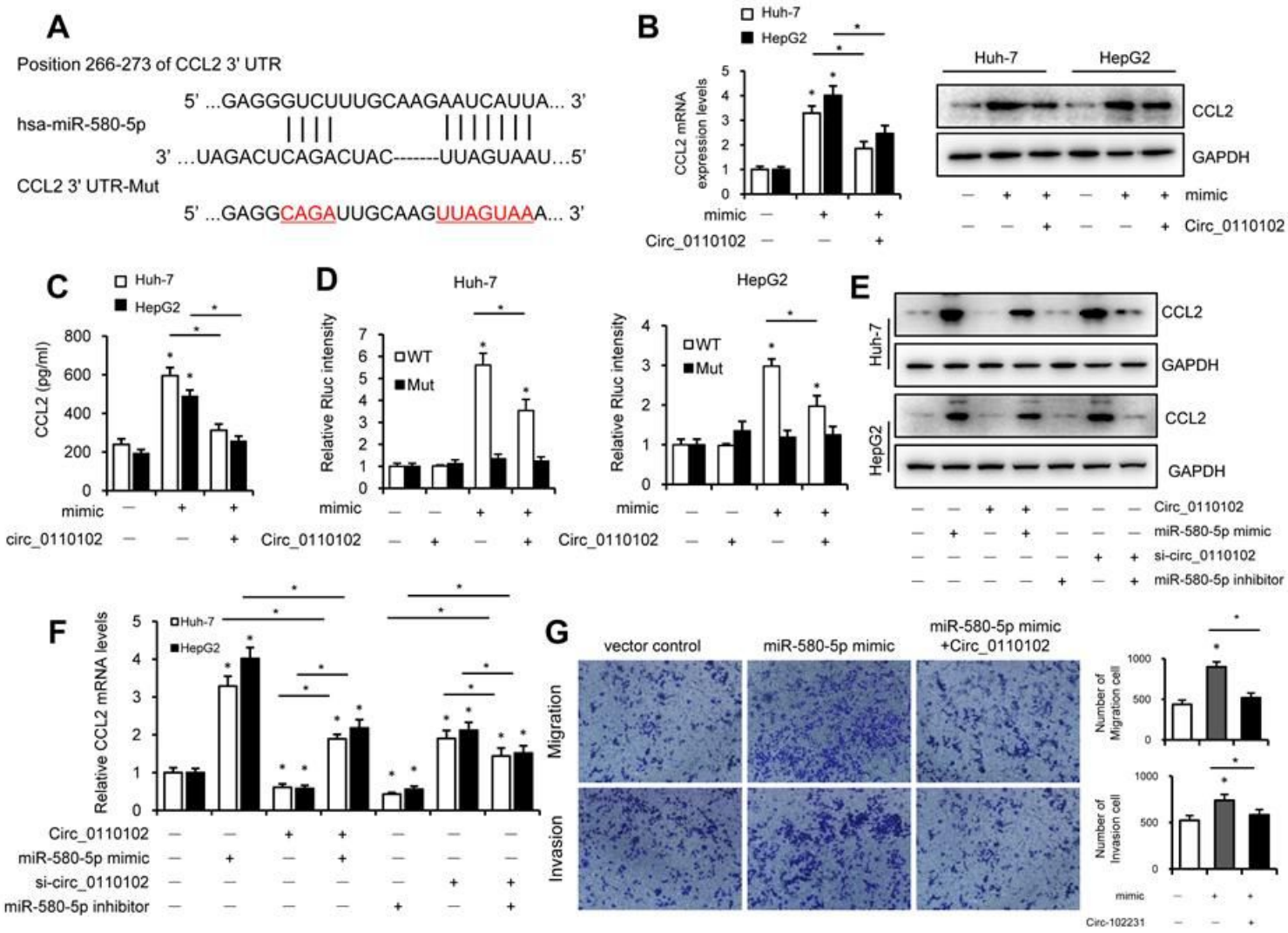

Figure 5

miR-580-5p induce CCL2 expression in HCC cells. (A) Predicted binding sites of miR-580-5p in the 3'-UTR of CCL2. (B-C) Huh-7 and HepG2 cells were co-transfected with miR-580-5p NC/mimic and hsa_circ-0110102 expression vector or vector control for 48 h. (B) CCL2 mRNA and protein levels were detected with RT-qPCR and western blot. (C) The contents of CCL2 in the medium were detected by ELISA. (D) Luciferase activity analysis was performed to detect luciferase activity in Huh-7 and HepG2 cells transfected with CCL2 3' UTR-WT or CCL2 3' UTR MUT plus with or without miR-580-5p or hsa_circ_0110102. (E-G) Huh-7 and HepG2 cells were transfected with miR-580-5p mimic or inhibitor, hsa_circ_0110102 expression vector or siRNA for 48 h. (E-F) CCL2 protein and mRNA levels were detected with western blot and RT-qPCR. (G) Cell migration and invasion were determined by Transwell assay. The representative magnified sections of Transwell cell staining images are shown. Statistical results based on three independent experiments. (200×). Data are presented as the mean ± S.E., *, P<0.05.

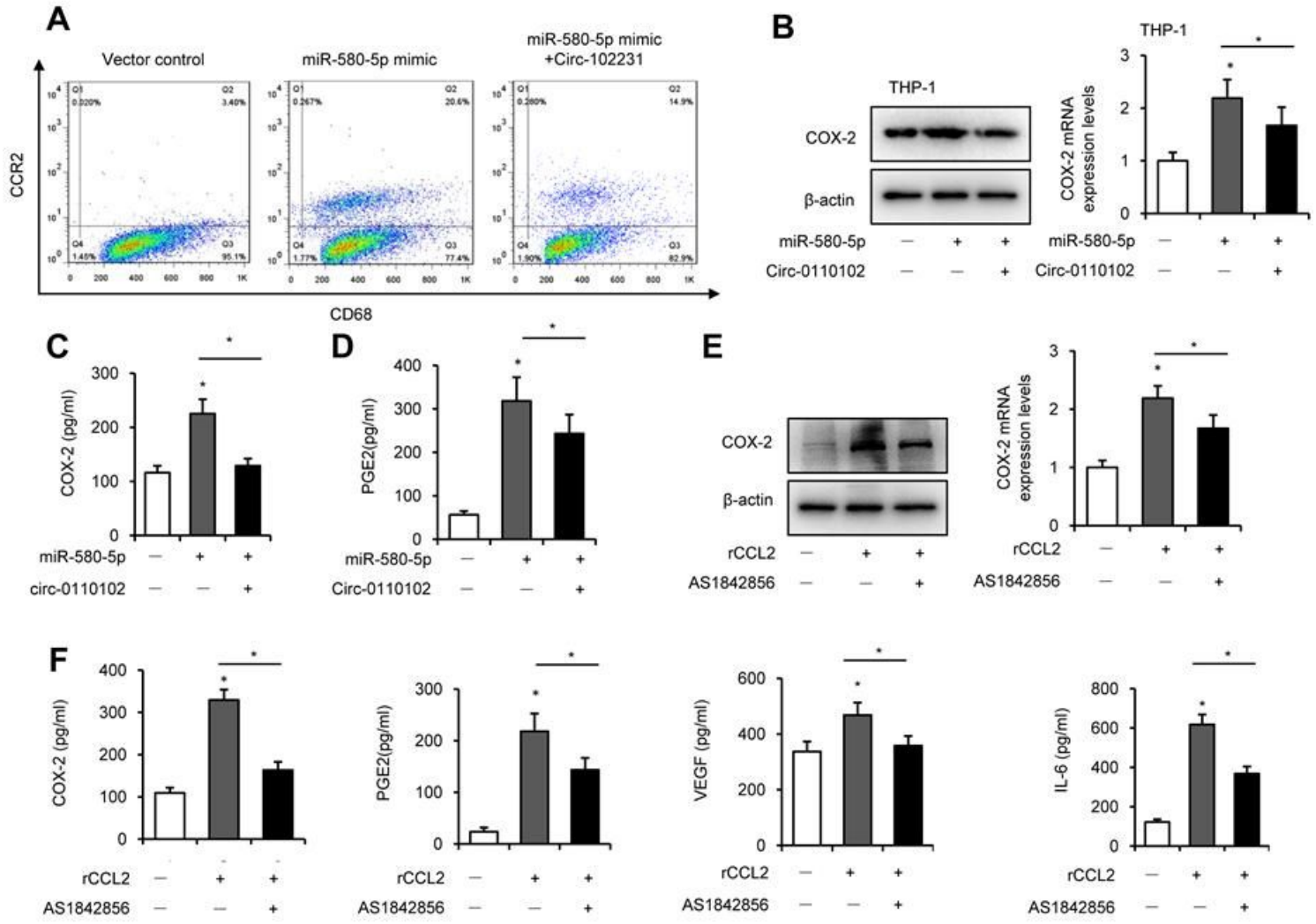

Figure 6

CCL2 induce COX-2 expression via FoxO1. Huh-7 cells were transfected with miR-580-5p mimic or hsa_circ_0110102, then co-cultured with THP-1 cells for 24 h. (A) THP-1 cells were incubated with CD68 and CCR2 antibodies, followed with flow cytometric to analysis the CCR2 expression. (B) CCL2 protein and mRNA levels in THP-1 cells were detected with RT-qPCR and western blot. (C-D) The contents of CCL2 and PGE2 in the supernatant of medium were measured using ELISA. (E-F) THP-1 cells were treated with 50 ng/ml rCCL2 and 1 μM AS1842856 for 48 h. (E) The COX-2 protein and mRNA levels were detected with RT-qPCR and western blot. (F) the contents of COX-2, PGE2, VEGF and IL-6 in the supernatant of medium were measured using ELISA. Data are presented as the mean ± S.E., *, P<0.05.

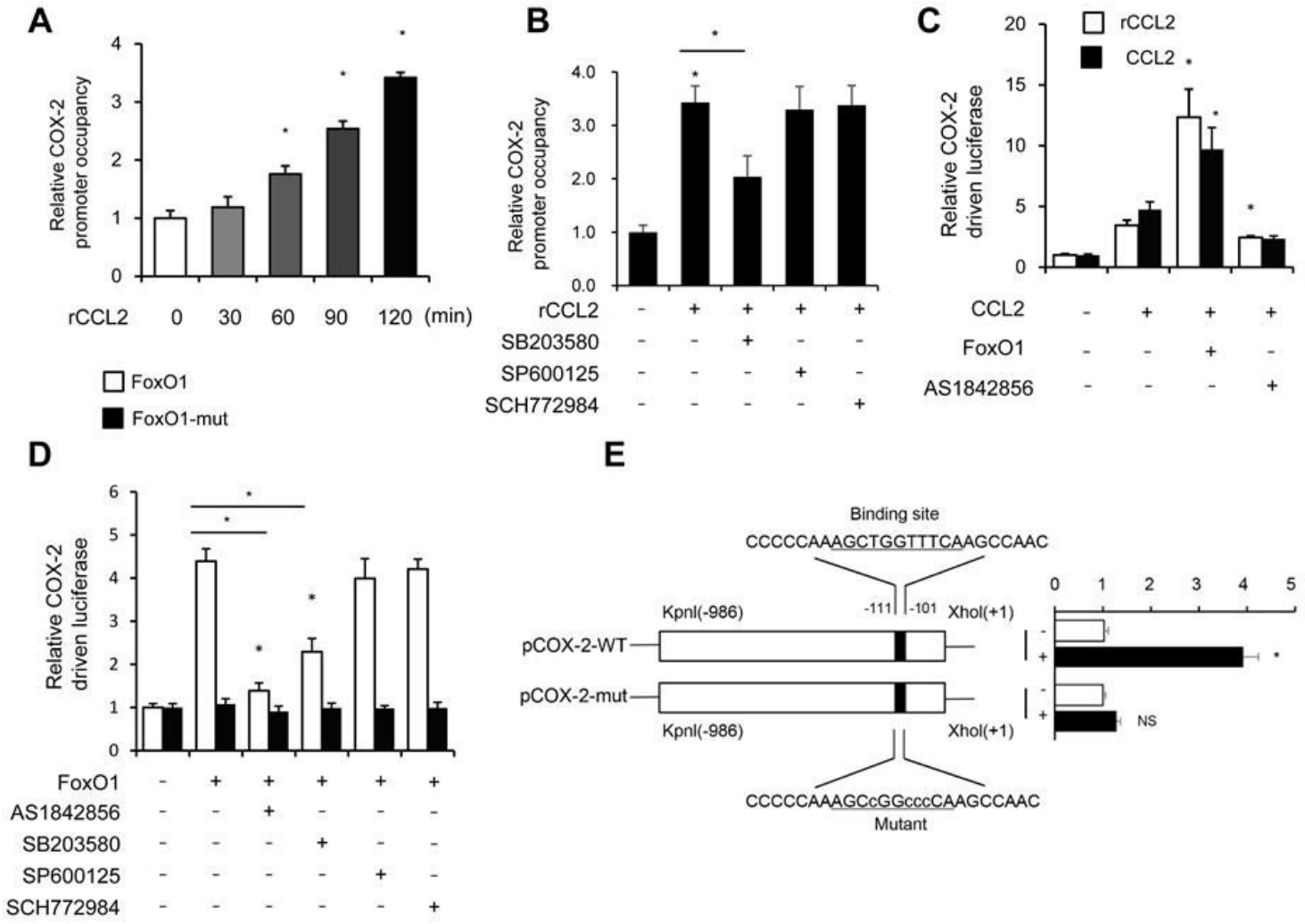

Figure 7

CCL2 induces FoxO1 activation via p38 MAPK dependent manner. (A-B) THP-1 were incubated with rCCL2 (50 ng/ml) for the indicated time intervals or pretreated with 10 μM SB203580, 10 μM SP600125 or 50 nM SCH772984 for 24 h, and then incubated with rCCL2 (50 ng/ml) for 120 min. ChIP assay was applied to examine the enrichment of FoxO1 onto COX-2 promoter. (C-D) THP-1 cells were transfected with FoxO1 expression vectors (50 ng), and pGL3-COX-2 (COX-2 promoter driven luciferase) construct (200 ng) plus pRL-TK-Renilla (10 ng). 36 h later, cells were treated with or without AS1842856 (1 μM) or plus 10 μM SB203580, 10 μM SP600125 or 50 nM SCH772984 for further 24 h. (E) THP-1 cells were co-transfected with wild-type COX-2 promoter reporter gene (Luc-COX-2-WT) or FoxO1 binding site-mutated COX-2 promoter reporter gene (Luc-COX-2-mut) with FoxO1. The COX-2 promoter activity was determined. Luciferase activity was normalized by Renilla luciferase values. Data are expressed as fold-change relative to the level of control. Data were presented as mean ± S.E., *, P<0.05.

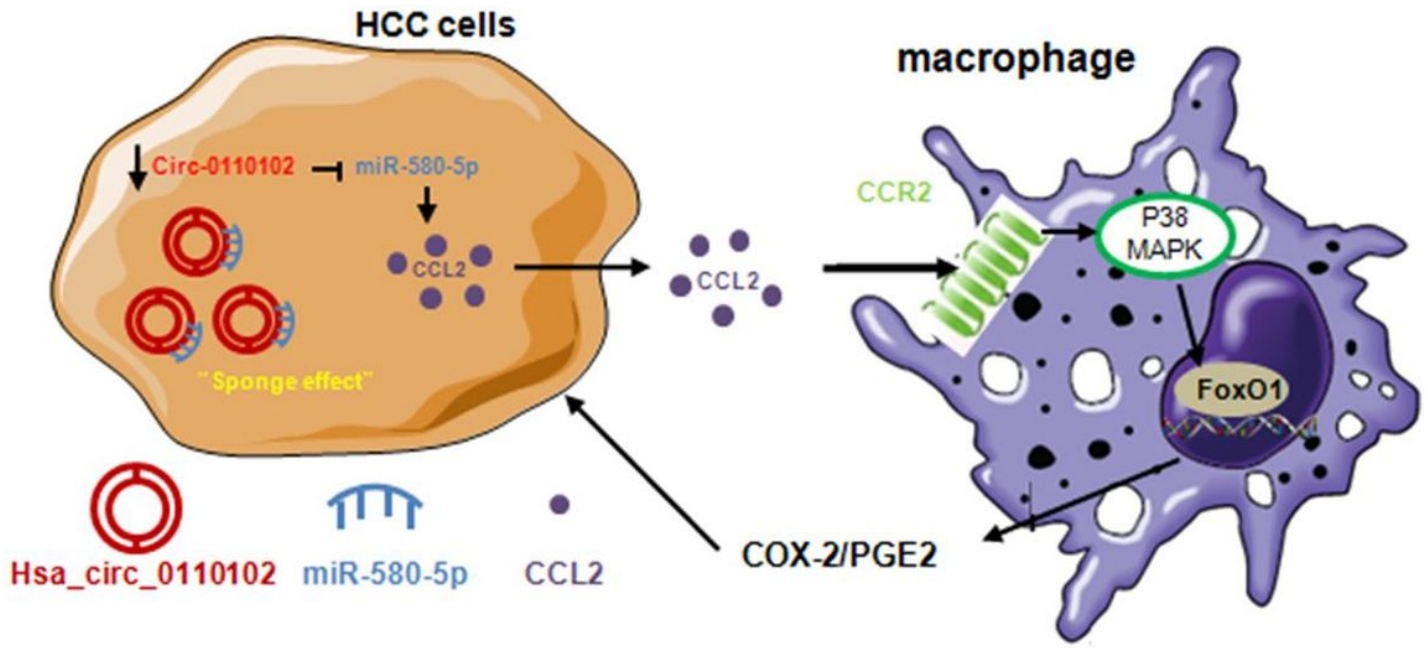

Figure 8

The proposed model illustrates the role of hsa_circ_0110102/miR-580-5p/CCL2 signaling in the regulation of HCC metastasis. hsa_circ_0110102 is down regulated in HCC patients with metastasis or recurrence and binds miR-580-5p, which target CCL2. CCL2 in the tumor microenvironment could active the COX-2/PGE2 pathway in macrophage via p38 MAPK/FoxO1 dependent manner.

Supplementary Files

This is a list of supplementary files associated with this preprint. Click to download.

- Originaldataforwesternblot.pdf
- SupplementaryInformation.docx